PIC SIMULATION OF NONLINEAR REGIME WAKE FIELD EXCITATION IN CYLINDRICAL RESONATOR

P.I. Markov, I.N. Onishchenko, A.F. Korzh, G.V. Sotnikov
National Science Center "Kharkov Institute of Physics and Technology"
Kharkov, Ukraine
E-mail: pmarkov@kipt.kharkov.ua

The nonlinear mechanism of saturation of wake field amplitude, exited in the cylindrical resonator partially filled with dielectric by relativistic train of electron bunches numerically simulated by means of a specially elaborated 2.5-dimensional electromagnetic PIC-code.

PACS: 02.60.Cb, 07.05.Tp

1. INTRODUCTION

The wakefield amplitude excited by a long train of electron bunches in dielectric waveguide is restricted, firstly, by attenuation due to low Q-factor of the resonator and, secondly, by nonlinear wave-particle interaction resulting in driver-beam trapping in the potential well of the wake. In this presentation the second mechanism of wakefield amplitude restriction is analyzed.

2. A STATEMENT OF PROBLEM

The investigation of a nonlinear stage of the slow wave excitation in the resonator by charged particles bunches (by a train of point electron bunches) was firstly considered in the paper [1]. Maximum attainable amplitude of an electric field was found to be not depended on a beam current and the number of injected bunches for obtaining amplitude saturation is inversely depended on beam current.

At present along with analytical methods of research there is a possibility of carrying out the detailed numerical simulation. In this presentation by means of a specially elaborated 2.5-dimensional electromagnetic PIC-code the excitation of electromagnetic field by a train of electron bunches in the cylindrical resonator partially filled with dielectric was simulated.

The geometry of a calculated model is depicted in the Fig.1. A statement of the problem is the following.

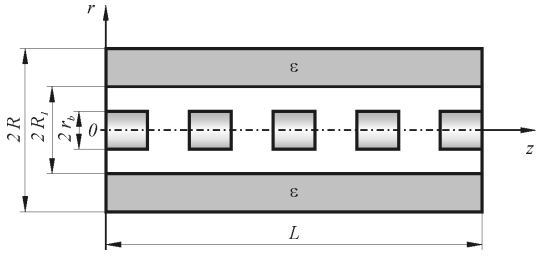

Fig.1. Geometry of a design model

The train of relativistic electron bunches is injected in the drift chamber through the left-hand boundary of a drift chamber. The bunch radii is r_b. The average electron current is I_b. At the resonator input (at $z = 0$) injected bunch is monoenergetic. The transversal components of electron velocities are equal to zero.

The system is axially symmetrical. It allows being restricted to the solution of set of Maxwell equations

$$\frac{\partial E_r}{\partial t} = -c\frac{\partial H_\varphi}{\partial z} - 4\pi j_r;$$
$$\frac{\partial E_z}{\partial t} = \frac{c}{r}\frac{\partial}{\partial r}\left(r H_\varphi\right) - 4\pi j_z;$$
$$\frac{\partial H_\varphi}{\partial t} = c\left(\frac{\partial E_z}{\partial r} - \frac{\partial E_r}{\partial z}\right);$$
$$\frac{\partial E_\varphi}{\partial t} = c\left(\frac{\partial H_r}{\partial z} - \frac{\partial H_z}{\partial r}\right) - 4\pi j_\varphi;$$
$$\frac{\partial H_r}{\partial t} = c\frac{\partial E_\varphi}{\partial z};$$
$$\frac{\partial H_z}{\partial t} = -\frac{c}{r}\frac{\partial}{\partial r}\left(c E_\varphi\right),$$

where E_r, E_z, E_φ and H_r, H_z, H_φ are the components of electric and magnetic intensity in cylindrical coordinate system and j_r, j_z, j_φ are the components of current density in the drift region, at numerical simulation of dynamics of electromagnetic fields. They are calculated by means of the mechanism of «distribution» of currents in nodes of a two-dimensional spatial grid (Fig.2).

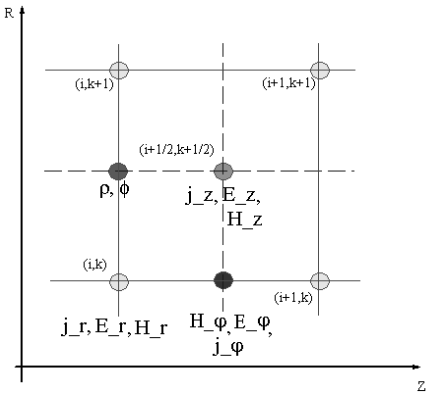

Fig.2. Spatial grid

Thus it is necessary to know a position and velocity of each macroparticle. They are determined from the solution of motion equations

$$\begin{cases} \ddot{r} = \beta\left[E_r - \dot{r}\delta + \left(r\dot{\varphi}B_z - \dot{z}B_\varphi\right)/c\right] + r\dot{\varphi}^2; \\ \ddot{\varphi} = \left\{\beta\left[E_\varphi - r\dot{\varphi}\delta + \left(\dot{z}B_r - \dot{r}B_z\right)/c\right] - 2\dot{r}\dot{\varphi}\right\}/r; \\ \ddot{z} = \beta\left[E_z - \dot{z}\delta + \left(\dot{r}B_\varphi - r\dot{\varphi}B_r\right)/c\right], \end{cases}$$

where

$$\beta = q\sqrt{1-v^2/c^2}\,\Big/ m,\ v^2 = (\dot r)^2 + (r\dot\varphi)^2 + (\dot z)^2;$$

$$\delta = \left(\dot r E_r + r\dot\varphi E_\varphi + \dot z E_z\right)\Big/ c^2;$$

$$B_z = B_{z0} + H_z;\ B_r = B_{r0} + H_r.$$

The numerical solution of Maxwell equations and «distribution» of charges were carried out on shifted one from other spatial (Fig.2) and time (Fig.3) grids.

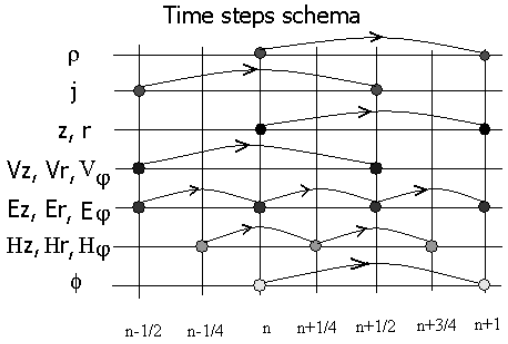

Fig.3. Time grid

For a time discretization of motion equations the predictor-corrector method was used. Values of the macroparticles velocities are calculated in half-integer points of time $t^{n+1/2} = (n+1/2)\tau$, and coordinates (z_p, r_p) — in the integer points of time $t^n = n\tau$ (n is integer, τ is a time step). Thus the values of the fields components, contained in the motion equations, are calculated by the linear interpolation from nodes of a grid. Owing to the selected plan, the solution of Maxwell equations is necessary to carry out twice more often, than solution of motion equations. Magnetic field H_φ is calculated in points of time $t^{n\pm1/4}$, and E_z and E_r in points of time t^n and $t^{n+1/2}$ respectively.

Boundary conditions for fields consists in referencing to zero of tangential components of an electromagnetic field on walls of the drift chamber. At an initial point of time the value of electromagnetic fields components are equal to zero; particles in the resonator are absent.

3. THE NUMERICAL ALGORITHM

In the issue the operations flowchart on one time step $\tau = t^{n+1} - t^n$ looks like this:

1. Finding the value of a magnetic field $H_r^{n+1/4}$, $H_z^{n+1/4}$, $H_\varphi^{n+1/4}$ at time step $t^{n+1/4}$

$$H_r^{n+1/4} = F_{H_r}\left(H_r^{n-1/4}, E_\varphi^n\right);$$

$$H_z^{n+1/4} = F_{H_z}\left(H_z^{n-1/4}, E_\varphi^n\right);$$

$$H_\varphi^{n+1/4} = F_{H_\varphi}\left(H_\varphi^{n-1/4}, E_r^n, E_z^n\right).$$

2. Calculation the values of components of electric biasing vector $D_r^{n+1/2}$, $D_z^{n+1/2}$ and $D_\varphi^{n+1/2}$ at time step $t^{n+1/2}$

$$D_r^{n+1/2} = F_{D_r}\left(D_r^n, H_\varphi^{n+1/4}, j_r^{n-1/2}\right);$$

$$D_z^{n+1/2} = F_{D_z}\left(D_z^n, H_\varphi^{n+1/4}, j_z^{n-1/2}\right);$$

$$D_\varphi^{n+1/2} = F_{D_\varphi}\left(D_\varphi^n, H_r^{n+1/4}, H_z^{n+1/4}, j_\varphi^{n-1/2}\right).$$

3. Calculation the values of components of electric field $E_r^{n+1/2}$, $E_z^{n+1/2}$ and $E_\varphi^{n+1/2}$ at time step $t^{n+1/2}$

$$E_{r_{j,i}}^{n+1/2} = D_{r_{j,i}}^{n+1/2}\Big/\varepsilon_{r_{j,i}},$$

$$E_{z_{j+1/2,i+1/2}}^{n+1/2} = D_{z_{j+1/2,+1/2i}}^{n+1/2}\Big/\varepsilon_{z_{j+1/2,i+1/2}},$$

$$E_{\varphi_{j+1/2,i}}^{n+1/2} = D_{\varphi_{j+1/2,i}}^{n+1/2}\Big/\varepsilon_{\varphi_{j+1/2,i}}.$$

4. Finding the value of a magnetic field $H_r^{n+3/4}$, $H_z^{n+3/4}$, $H_\varphi^{n+3/4}$ at time step $t^{n+3/4}$

$$H_r^{n+3/4} = F_{H_r}\left(H_r^{n+1/4}, E_\varphi^{n+1/2}\right);$$

$$H_z^{n+3/4} = F_{H_z}\left(H_z^{n+1/4}, E_\varphi^{n+1/2}\right);$$

$$H_\varphi^{n+3/4} = F_{H_\varphi}\left(H_\varphi^{n+1/4}, E_r^{n+1/2}, E_z^{n+1/2}\right).$$

Finding the value of a magnetic field $H_r^{n+1/2}$, $H_z^{n+1/2}, H_\varphi^{n+1/2}$ at time step $t^{n+1/2}$ by averaging

$$H_{r_{j,i}}^{n+1/2} = \left(H_{r_{j,i}}^{n+1/4} + H_{r_{j,i}}^{n+3/4}\right)\Big/2,$$

$$H_{z_{j+1/2,i+1/2}}^{n+1/2} = \left(H_{z_{j+1/2,i+1/2}}^{n+1/4} + H_{z_{j+1/2,i+1/2}}^{n+3/4}\right)\Big/2,$$

$$H_{\varphi_{j+1/2,i}}^{n+1/2} = \left(H_{\varphi_{j+1/2,i}}^{n+1/4} + H_{\varphi_{j+1/2,i}}^{n+3/4}\right)\Big/2.$$

5. Solving of motion equations by the predictor-corrector method:
   a. calculation a preliminary value of an angular velocity of macroparticle $\omega^{n+1/2}$;
   b. the values of r^{n+1}, z^{n+1}, v_r^{n+1}, v_z^{n+1};
   c. finding the values of the same quantities at time step $t^{n+1/2}$ by averaging;
   d. calculation a final value of an angular velocity of macroparticle $\omega^{n+1/2}$.
6. Calculating values of a current density j_z, j_r and j_φ in grid nodes for time step $t^{n+1/2}$.
7. Injecting new macroparticles in the drift chamber.
8. Computing the values of a charge density of ρ for time step t^{n+1}.
9. Calculation the values a components of electric biasing vector D_r^{n+1}, D_z^{n+1} and D_φ^{n+1} at time step t^{n+1}

$$D_r^{n+1} = F_{D_r}\left(D_r^{n+1/2}, H_\varphi^{n+3/4}, j_r^{n+1/2}\right);$$

$$D_z^{n+1} = F_{D_z}\left(D_z^{n+1/2}, H_\varphi^{n+3/4}, j_z^{n+1/2}\right);$$

$$D_\varphi^{n+1} = F_{D_\varphi}\left(D_\varphi^{n+1/2}, H_r^{n+3/4}, H_z^{n+3/4}, j_\varphi^{n+1/2}\right).$$

10. Calculation the values of components of electric field E_r^{n+1}, E_z^{n+1} and E_φ^{n+1} at time step t^{n+1}

$$E_{r\,j,i}^{n+1} = D_{r\,j,i}^{n+1} \Big/ \varepsilon_{r\,j,i},$$
$$E_{z\,j+1/2,i+1/2}^{n+1} = D_{z\,j+1/2,+1/2i}^{n+1/2} \Big/ \varepsilon_{z\,j+1/2,i+1/2},$$
$$E_{\varphi\,j+1/2,i}^{n+1} = D_{\varphi\,j+1/2,i}^{n+1} \Big/ \varepsilon_{\varphi\,j+1/2,i}.$$

11. Carrying-out the correction of an electric field E_z and E_r for time step t^{n+1} according to the Boris scheme

$$\vec{\boldsymbol{E}} = \vec{\boldsymbol{E}}^{*} - \nabla_D \delta\Phi,$$

where $\vec{\boldsymbol{E}}^{*}$ and $\vec{\boldsymbol{E}}$ are initial and corrected electric field values, $\delta\Phi$ is correction to electric field potential, ∇_D is a difference analog of the Hamilton operator.

For preventing occurrence of electromagnetic field noise with grid period, on each ten-thousand step of evaluations the nine point fields averaging was fulfilled.

3. RESULTS OF NUMERICAL SIMULATION

The algorithm described above has been implemented as a complex of C ++ programs. The main parameters were chosen close to existing ones in the installation "Almaz-2", namely, the radius of the drift chamber is 4.3 cm, permittivity is equal 2.1, radius of the channel for beam in dielectric is 1.05 cm, length of the chamber is 55.3 cm, electron bunch radius is 0.5 cm, electron energy is 5 MeV, bunch duration is 0.078 ns, pulse repetition period is 0.37 ns. For reduction of calculating time and numerical errors the average injected current was chosen 10 A, i.e. 20 times greater than experimental value.

Results of simulation showed that during the first 85.5 ns, i.e. when 230 bunches were injected practically linear growth of electric field amplitude up to saturation value of 95 kV/cm is observed (see Fig.4). We assume that the expected number of clots at current of 0.5 A is about 4600.

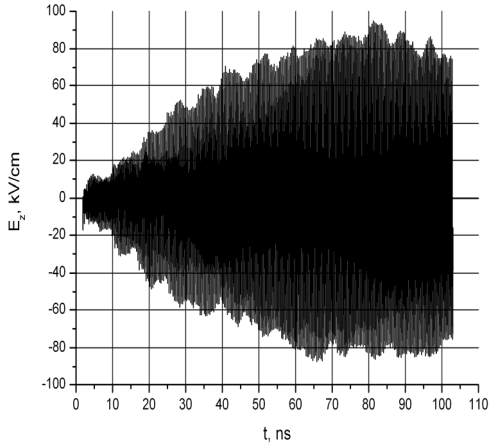

Fig.4. Time dependence of intensity of an electric field on an axis at a right end face of the resonator

The electric field spectrum corresponding to Fig.4 is depicted on Fig.5. It's visible, that the basic maximum on an electric field oscillation spectrum has frequency 2.7 GHz. More high-frequency maximums with amplitude approximately 10 times smaller are spread up to frequency 16.2 GHz.

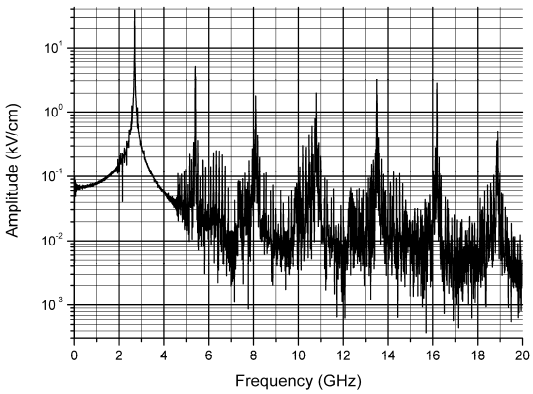

Fig.5. The electric field spectrum

Linear growth of field amplitude results in square-law change of field energy that it is possible to see on the energy diagram (Fig.6). We shall notice a good performance of the energy conservation law in our simulation.

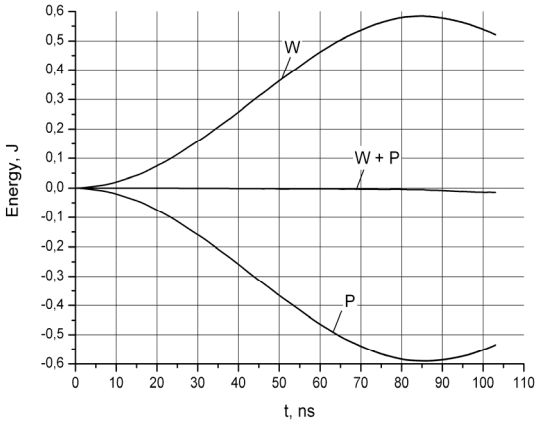

Fig.6. The energy diagram: W is the electromagnetic field energy, P is the particles energy losses

After achieving of maximum the electric field amplitude oscillates slowly with frequency of about 11 MHz. Self-consistent influence of excited field on bunches motion dynamics leads to essential spreading of longitudinal and transversal velocities of electrons on the phase plane (see Fid. 7, where spreading of longitudinal velocities is depicted).

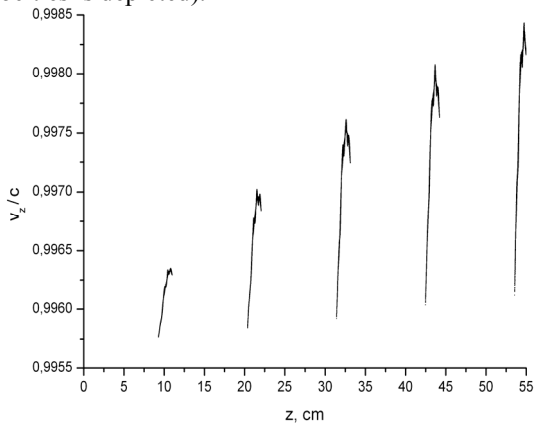

Fig.7. Phase plane for macroelectrons

Despite of essential spread of particles on velocities, their relativistic factor remains high. Therefore in configuration space the spread of particles is observed only on cross coordinate, while shift of particles in a longitudinal direction is absent, that it is possible to view in Fig.8.

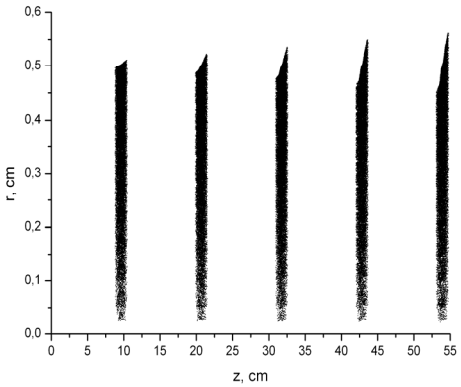

Fig.8. Configuration space for macroelectrons

CONCLUSIONS

The executed numerical simulation has shown, that nonlinear trapping processes caused by back influence of field of big amplitude on charged bunches, result in restriction of amplitude of an electric field in system. Time of field amplitude growth, and its value are received. The number of electron bunches which should be injected in the resonator for achievement of a maximum of a field is estimated.

This study was partly supported by CRDF Grant # UP2-2569-KH-04.

REFERENCES

1. V.I. Kurilko, J. Ullschmied // *Nuclear Fusion.* 1969. №9, p.129-135.
2. V.A. Balakirev, I.N. Onishchenko, D.Yu. Sidorenko, G.V. Sotnikov // *Pisma v JTF.* 2003, v.29, №14, p.39-45 (in Russian).

МОДЕЛИРОВАНИЕ НЕЛИНЕЙНОГО РЕЖИМА ВОЗБУЖДЕНИЯ КИЛЬВАТЕРНОГО ПОЛЯ В ЦИЛИНДРИЧЕСКОМ РЕЗОНАТОРЕ С ПОМОЩЬЮ PIC-КОДА

П.И. Марков, И.Н. Онищенко, А.Ф. Корж, Г.В. Сотников

С помощью специально разработанного нами 2.5-мерного электромагнитного PIC–кода численно промоделирован нелинейный механизм ограничения амплитуды кильватерного поля, возбуждаемого в цилиндрическом резонаторе, частично заполненном диэлектриком, релятивистской последовательностью электронных сгустков. Моделирование показало, что нелинейные захватные процессы, вызванные обратным влиянием поля большой амплитуды на заряженные сгустки, приводят к ограничению амплитуды электрического поля в системе. Получено время нарастания амплитуды поля, его амплитуда. Оценено количество электронных сгустков, которые следует инжектировать в резонатор для достижения максимума поля.

МОДЕЛЮВАННЯ НЕЛІНІЙНОГО РЕЖИМУ ЗБУДЖЕННЯ КІЛЬВАТЕРНОГО ПОЛЯ В ЦИЛІНДРИЧНОМУ РЕЗОНАТОРІ ЗА ДОПОМОГОЮ PIC-КОДУ

П.І. Марков, І.М. Онищенко, О.Ф. Корж, Г.В. Сотніков

За допомогою спеціально розробленого нами 2.5-мірного електромагнітного PIC-коду чисельно промодельовано нелінійний механізм обмеження амплітуди кільватерного поля, збуджуваного в циліндричному резонаторі, частково заповненому діелектриком, релятивістською послідовністю електронних згустків. Моделювання показало, що нелінійні захватні процеси, викликані зворотним впливом поля великої амплітуди на заряджені згустки, приводять до обмеження амплітуди електричного поля в системі. Отримано час наростання амплітуди поля, його амплітуду. Оцінено кількість електронних згустків, які слідує інжектувати у резонатор для досягнення максимуму поля.